

General Disclaimer

One or more of the Following Statements may affect this Document

- This document has been reproduced from the best copy furnished by the organizational source. It is being released in the interest of making available as much information as possible.
- This document may contain data, which exceeds the sheet parameters. It was furnished in this condition by the organizational source and is the best copy available.
- This document may contain tone-on-tone or color graphs, charts and/or pictures, which have been reproduced in black and white.
- This document is paginated as submitted by the original source.
- Portions of this document are not fully legible due to the historical nature of some of the material. However, it is the best reproduction available from the original submission.

CR 86290

INVESTIGATION OF REFRACTORY DIELECTRIC FOR INTEGRATED CIRCUITS

By. V.Y. Doo, P.J. Tsang, and P.C. Li

December 1968

Distribution of this report is provided in the interest of information exchange, and should not be construed as endorsement by NASA of the material presented. Responsibility for the contents resides with the organization that prepared it.

Prepared under Contract No. NAS 12-667 by

INTERNATIONAL BUSINESS MACHINES CORPORATION

Hopewell Junction, New York 12533

ELECTRONICS RESEARCH CENTER

NATIONAL AERONAUTICS AND SPACE ADMINISTRATION

CAMBRIDGE, MASSACHUSETTS

FACILITY FORM 802

N70-14289 (ACCESSION NUMBER)	(THRU)
23 (PAGES)	1
CR 86290 (NASA CR OR TMX OR AD NUMBER)	(CODE)
	09 (CATEGORY)



INVESTIGATION OF REFRACTORY DIELECTRIC FOR INTEGRATED CIRCUITS

By. V.Y. Doo, P.J. Tsang, and P.C. Li

December 1968

Prepared under Contract No. NAS 12-667 by
INTERNATIONAL BUSINESS MACHINES CORPORATION

Hopewell Junction, New York 12533

ELECTRONICS RESEARCH CENTER
NATIONAL AERONAUTICS AND SPACE ADMINISTRATION
CAMBRIDGE, MASSACHUSETTS

1.0 INTRODUCTION

This is the second quarterly report on Contract No. NAS 12-667, covering the work performed from September 1 to November 30, 1968. The objective of this contract is to conduct research and development on refractory dielectric for integrated circuits application. During this reporting period, investigation on the process development for chemical deposition of Al_2O_3 and film properties continued. In addition, the effect of SiO_2 sub-layer on the growth mode as well as the surface texture of the Al_2O_3 film on silicon wafer was studied. The masking ability of Al_2O_3 film against the permeation of various doping elements including Ga, B, and P was investigated. A great deal of effort was devoted to the study of C-V characteristics of the films including Al_2O_3 films on bare silicon and on SiC_2 coated silicon wafers. Property measurements on the Al_2O_3 films included flat band voltage, charge density, and the turn-on voltage using MOS techniques.¹ Some modification of the existing deposition system was made to enable an in-situ growth of SiO_2 prior to the Al_2O_3 deposition. Electrical properties of this type film were measured and compared with those containing SiO_2 sub-layers prepared by other methods. For better characterization, the morphology of Al_2O_3 was further studied using scanning electron microscope. Results are presented in this report.

2.0 PYROLYTIC ALUMINA ACHIEVEMENTS

2.1 ADDITIONAL STUDY ON THE GROWTH MODE OF Al_2O_3 FILMS

For integrated circuits application, the dielectric films must be physically homogeneous and free from pin holes or structural defects, all of which can cause device instability. It is highly desirable to have a film of single phase so that the film properties, both physical and chemical, can maintain uniformity in every micro-spot. This requirement is extremely important to the reliability of electronic device.

Some preliminary results of Al_2O_3 film growth by chemical vapor deposition were reported in the first quarterly report.² Because of the importance of the film quality required in electronic application, additional study of the film growth mode was conducted during this period with the goal to achieve the best process conditions for film preparation. In particular, important process parameters pertinent to film growth were studied carefully. Those include substrate temperature, $\text{CO}_2/\text{AlCl}_3$ mole ratio, and carrier gas.

2.1.1 Growth Mode and Rate of Al_2O_3 Film as a Function of $\text{CO}_2/\text{AlCl}_3$ Mole Ratio

The growth mode and rate of Al_2O_3 film were studied at 900°C as a function of the $\text{CO}_2/\text{AlCl}_3$ mole ratio. This temperature was chosen because of the γ phase Al_2O_3 formation in the film as identified by previous observation.² By maintaining constant flow rates of main carrier gas (H_2) and the carrier gas for AlCl_3 (H_2) (20 l/min and 500 cc/min, respectively), the $\text{CO}_2/\text{AlCl}_3$ mole ratio was varied from 15:1 to 90:1 by changing the CO_2 flow rate.

Experimental results are presented in Fig. 1, in which the film growth rate steadily increases with an increasing $\text{CO}_2/\text{AlCl}_3$ mole ratio. The Al_2O_3 films thus prepared were visually clear, indicating a single mode of growth. However, if the $\text{CO}_2/\text{AlCl}_3$ ratio is increased excessively, a bimodal film may develop. When excess CO_2 is contained in the gas phase, the amount of water formed can be sufficiently high to cause pronounced Al_2O_3 formation in the gas phase rather than on the substrate surface. Experience from experimental observation indicates that the ratio of $\text{CO}_2/\text{AlCl}_3$ at 20:1 appears most satisfactory in the existing system.

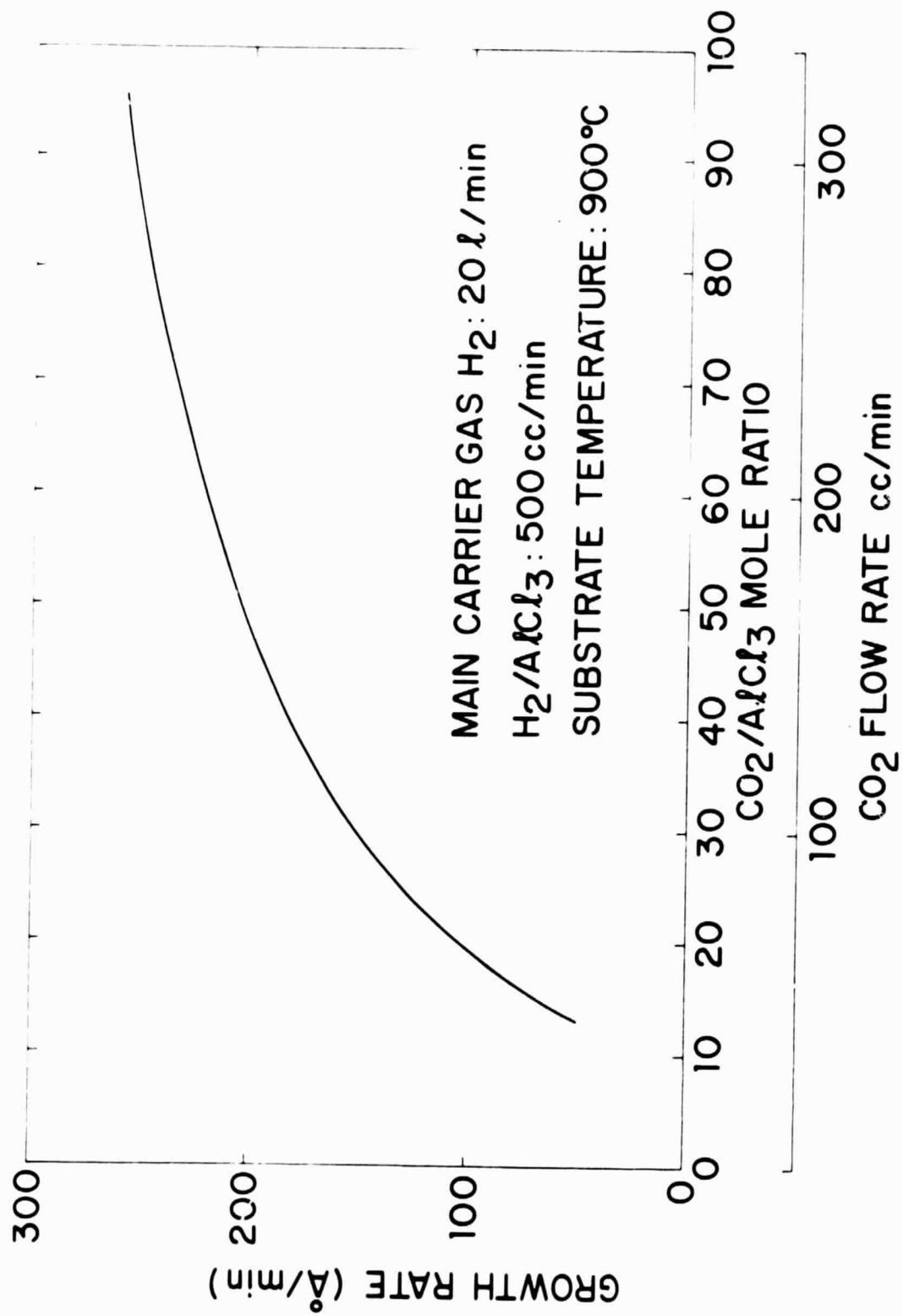


Fig. 1. Effect of CO₂/AlCl₃ mole ratio on the growth of Al₂O₃ film on silicon wafer.

2.1.2 High Temperature Film Growth

To further identify the growth mode with respect to temperature, a number of experiments on film growth were conducted at temperatures above 900°C . It was found that as the substrate temperature was raised above 900°C , surface nebulosity developed. Microscopic observation revealed that these high temperature films were not homogeneous in morphology. One of the possible reasons would be a premature chemical reaction taking place in the gas phase and forming some Al_2O_3 soot which would be continuously entrapped into the film during the growth. Consequently, a film of multimodal growth is produced. At 950°C substrate temperature, films of multimodal growth can be well identified. When the substrate temperature was increased further, say above 1050°C , coarse grains resulting from grain growth rapidly developed in such multimodal films. It is evident that 900°C is the most satisfactory temperature from the viewpoint of growth mode for Al_2O_3 films.

2.1.3 The Ratio of Main Carrier Gas Over AlCl_3 Carrier Gas

The ratio of main carrier gas over AlCl_3 carrier gas is another factor to control the reaction rate. The higher the main carrier gas flow rate, the less the concentration of AlCl_3 in the gas phase. At 900°C , the satisfactory ratio of main carrier gas over AlCl_3 carrier gas is approximately 30:1 when the AlCl_3 vaporized at 115°C . If the substrate is heated to a higher temperature, this ratio must be increased correspondingly, otherwise a single modal film growth would not be maintained. This is illustrated by the following example. At 1000°C and $\text{CO}_2/\text{AlCl}_3 = 18:1$, the Al_2O_3 film prepared was found to be of multimodal growth under the ratio of main carrier gas over AlCl_3 carrier gas being less than 70. But when this ratio was doubled, the film appeared to be of single modal growth. Thus, it is important to properly dilute the AlCl_3 concentration to prevent any possible early formation of Al_2O_3 in the gas phase.

2.1.4 Effect of Argon Gas on the Growth of Al_2O_3 Film

A study was conducted by substituting the H_2 with A as the main carrier gas. It was found that the complete substitution of A for H_2 as the main carrier gas tends to decrease the film growth rate from $\sim 150 \text{ \AA}/\text{min.}$ to $\sim 20 \text{ \AA}/\text{min.}$, with other conditions unchanged.

When a mixture of H_2 and A was admitted as the main carrier gas, the growth rate of the Al_2O_3 film increased. Results indicated that the growth rate of Al_2O_3 film increases linearly with increasing H_2 concentrations in the gas phase as shown in Fig. 2. High A concentration appears to produce two effects. First, the gas phase reaction seems to be depressed; and second, the single modal growth is likely to extend to a higher substrate temperature. The stoichiometry of the Al_2O_3 may differ when using H_2 as the sole carrier gas. This sort of speculation needs additional experimental study. Results of C-V measurements indicate that the N_{FB} of the Al_2O_3 film grown in H_2 main carrier gas. This is discussed further in Section 2.4.1.

2.1.5 Structure of Al_2O_3 Films Deposited on SiO_2 - Coated and Bare Si Substrates

The structure and appearance of the Al_2O_3 films deposited on SiO_2 -coated Si substrates differed markedly from that on bare Si-substrates. The amorphous-crystalline phase transition temperature of the Al_2O_3 films deposited on SiO_2 -coated Si is higher than those deposited on bare Si because of the structural difference in substrates. For the same reason, single crystal Al_2O_3 film was never observed on SiO_2 -coated substrates even though preferential orientation has been found in some films.

The topograph of the Al_2O_3 films deposited at different temperatures on SiO_2 -coated and bare Si substrates was investigated by using the scanning electron

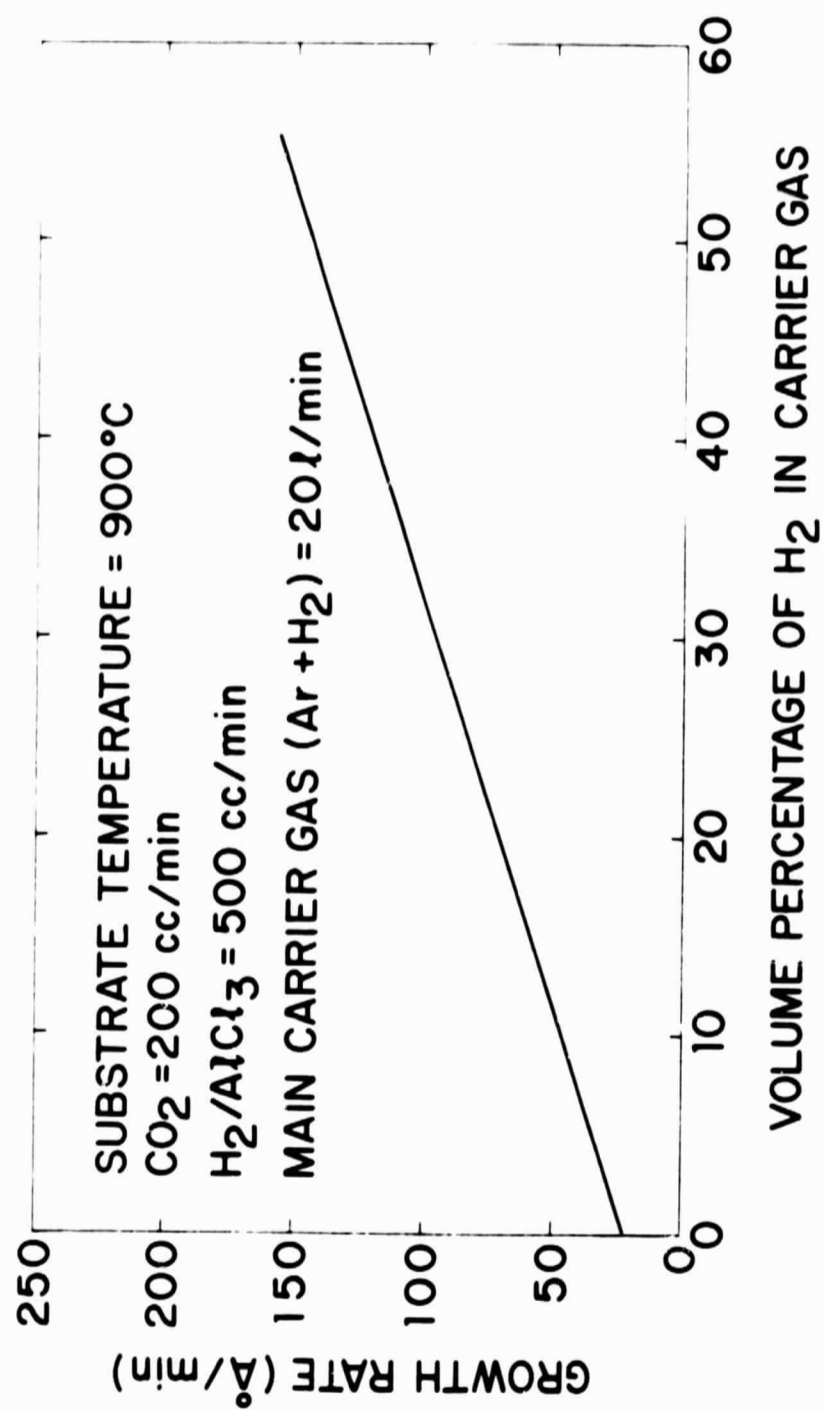


Fig. 2. Effect of composition of carrier gas on Al₂O₃ film growth.

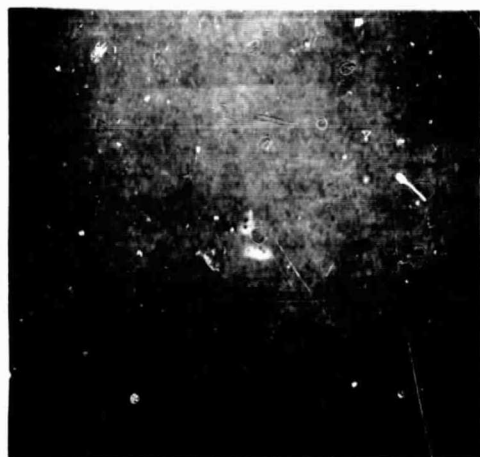
microscope, SEM. Samples a1, b1 and c1 were deposited on bare Si substrates and a2, b2, and c2 on SiO₂-coated substrates. The deposition temperature for samples a1 and a2 was 1050°C, b1 and b2 at 900°C, and c1 and c2 at 700°C. Figure 3 shows the SEM topograph magnification at 100 and Fig. 4 at 10,000. Note in Fig. 3, that all samples appear to be smooth. However, under high magnification, the topographs differed markedly from one sample to another. In general, high surface asperity was observed on films deposited at high temperature and on SiO₂-coated substrates. A sectional SEM micrograph of a 2.5μ film grown at 1100°C is shown in Fig. 5. Apparently, multimodal deposition occurred in this sample thereby forming a high degree of surface roughness. Its columnar grain structure is readily observable.

2.2 REACTOR MODIFICATION FOR IN-SITU OXIDATION

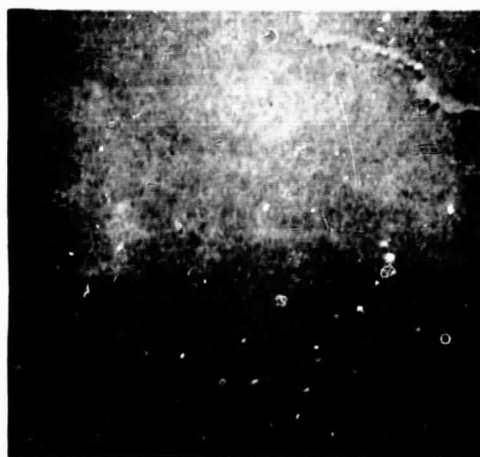
An earlier report on silicon nitride³ indicated that the interface property of the MNOS (Metal-Nitride-Oxide-Si) sample was the best when the oxide was grown in-situ. Therefore, it is interesting to see if the same effect will occur on the MAOS (Metal-Alumina-Oxide-Si) samples. In-situ oxidation demands reactor modification because the graphite susceptor for heating substrates will burn under an oxidizing atmosphere. To overcome this difficulty, the graphite susceptor was enclosed in quartz tubing. Dry oxygen was injected into the reactor through a separate line so that the AlCl₃-CO₂ lines are not contaminated.

2.3 DIFFUSION MASKING EFFECT

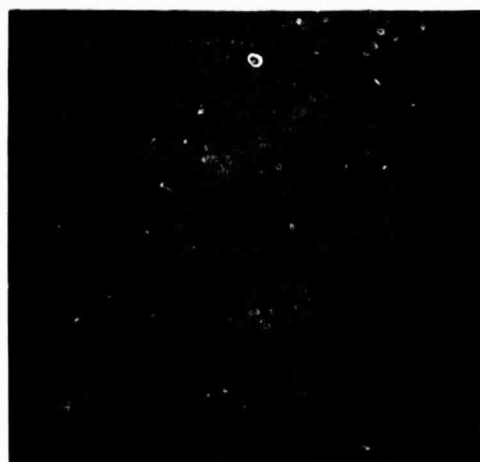
The masking effect of Al₂O₃ film prepared at 900°C against the diffusion of common dopants such as P, B, and Ga was investigated. Diffusion was carried out individually in sealed capsules for 70 minutes at 1050°C for P, 60 minutes at 1100°C for B, and 70 minutes at 1100°C for Ga. Diffused junction depth was determined by the bevel-delineation method. Several Al₂O₃ thicknesses were



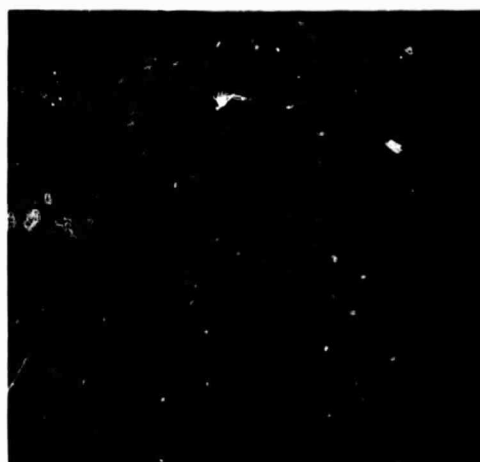
a1 A10-60-3 100X



a2 A10-60-6 100X



b1 A10-66-7 100X



b2 A10-66-6 100X

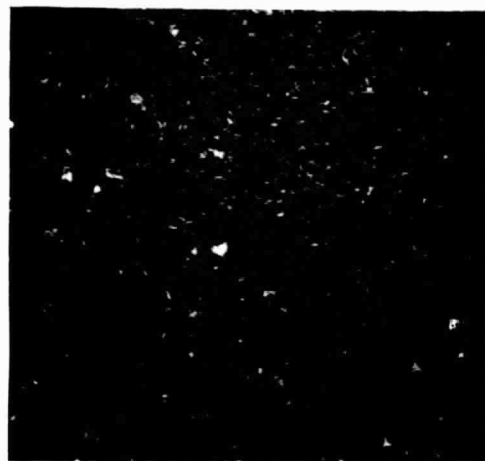


c1 A10-54-3 100X



c2 A10-54-7 100X

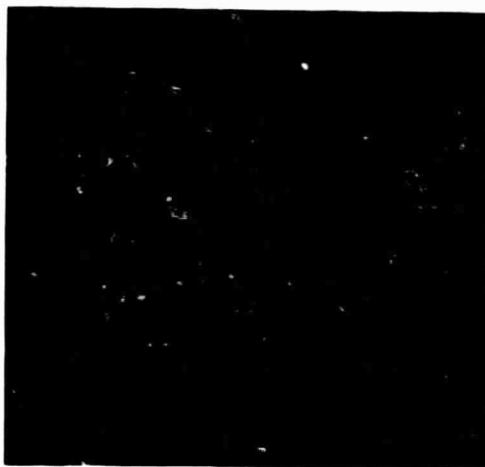
Fig. 3. SEM micrographs of the surface of Al_2O_3 films deposited at various temperatures. Magnifications X100. a1 and a2 deposited at 1050°C ; b1 and b2 deposited at 900°C ; c1 and c2 deposited at 700°C . a1, b1 and c1 without SiO_2 underlayer; a2, b2 and c2 with SiO_2 sublayer.



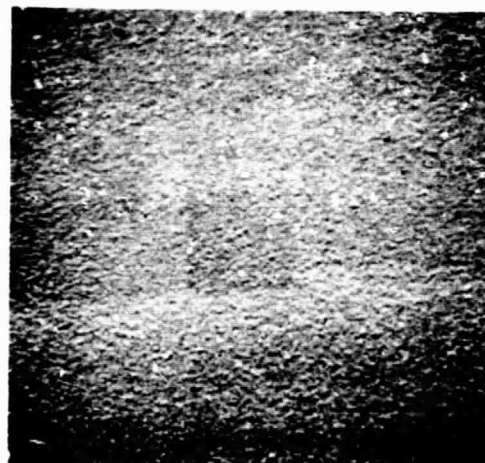
a1 AlO-60-3 10,000X



a2 AlO-60-6 10,000X



b1 AlO-66-7 10,000X



b2 AlO-66-6 10,000X



c1 AlO-54-3 10,000X

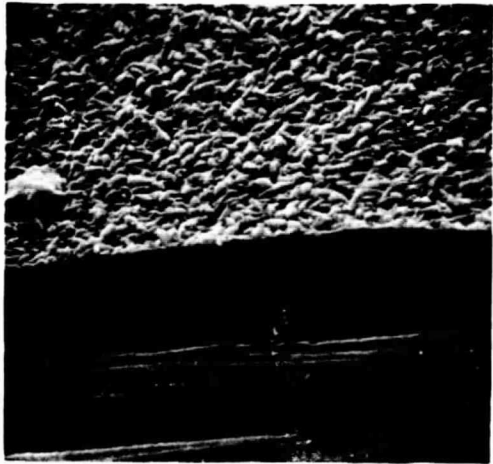


c2 AlO-54-7 10,000X

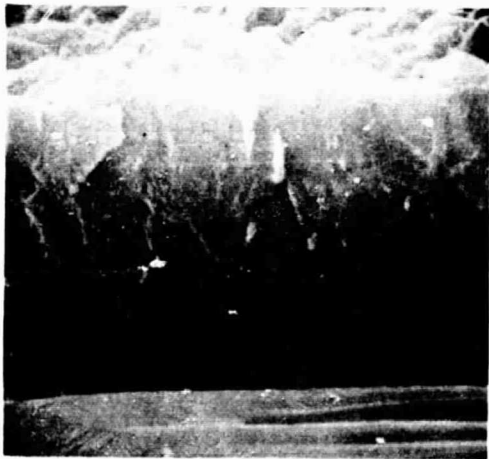
Fig. 4. SEM micrographs of the surface of Al_2O_3 films. Same as that shown in Fig. 4 but at much higher magnification: X10,000.
a1 and a2 deposited at 1050°C , b1 and b2 deposited at 900°C ; c1 and c2 deposited at 700°C .
a1, b1, and c1 without SiO_2 underlayer; a2, b2, and c2 with SiO_2 underlayer.



A10-80 200X



A10-80 2400X



A10-80 12,000X

Fig. 5. SEM micrographs of the cross-section of a thick Al₂O₃ film deposited at 1100°C.

used for each diffusion species. The results are shown in Fig. 6. The Al_2O_3 , effectively masked P-diffusion but not the B- & Ga-diffusion. Thick Al_2O_3 films did not help mask B- & Ga-diffusion because thick films tend to have a well defined columnar grain structure. The preferred grain boundary diffusion suggested a rugged junction as shown in Fig. 6.

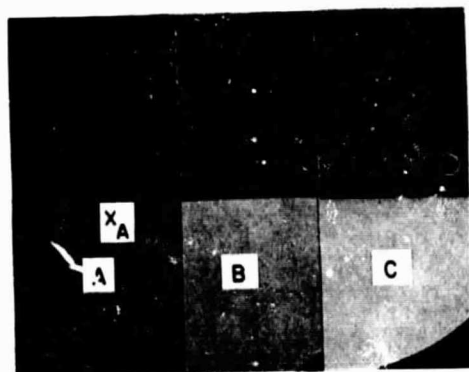
2.4 ELECTRICAL PROPERTIES EVALUATION

Surface charge density, flat band voltage, and dielectric constants of MAS (Metal-Aluminum Si) samples and the MAOS samples were determined by C-V measurements.¹ Regardless of the original wafer type, it was found that in the MAS samples, Al_2O_3 tends to make the surface silicon more P-type. This finding is in agreement with the results obtained by Aboaf⁴ and Matsushita and Koga.⁵ Similarly, thermally grown SiO_2 tends to make the silicon surface more N-type. Consequently, a double layered film composed of Al_2O_3 and thermal SiO_2 on silicon wafer would possibly make the surface either N- or P-type, depending upon the combined thickness of SiO_2 and Al_2O_3 . Preliminary results confirmed this trend, but additional study is needed to make it more conclusive.

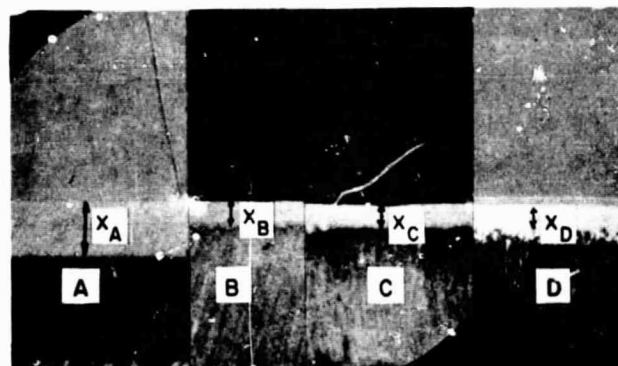
2.4.1 Room Temperature C-V Curves and Flat Band Charge Density of MAS Sample

2.4.1.1 Effect of Substrate Temperature

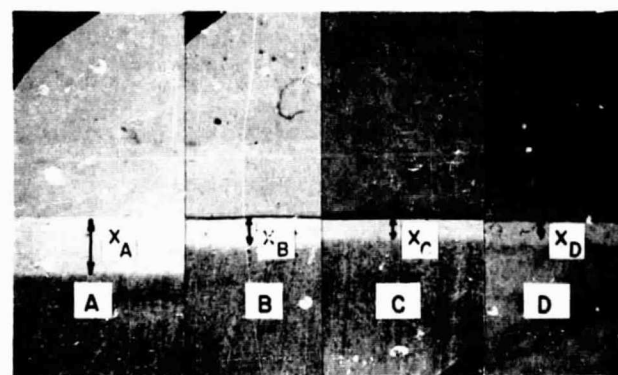
A typical C-V curve of Al_2O_3 on P-Si wafer is shown in Fig. 7. The positive V_{FB} is indicative of a "p-inverted" silicon surface. The C-V curves are fairly stable at room temperature and exhibit only minor hysteresis. Depending on the bias sweep speed, the magnitude of hysteresis, ΔV_{h} becomes so small to be measurable practically.



P DIFFUSION
 $X_A = 1.96 \mu$



Ga DIFFUSION
 $X_A = 2.4 \mu; X_B = 1.19 \mu; X_C = 1.13 \mu; X_D = 1.20 \mu$



B DIFFUSION
 $X_A = 2.6 \mu; X_B = 1.23 \mu; X_C = 1.37 \mu; X_D = 1.35 \mu$

Fig. 6. Microphotographs of the beveled and stained cross-section of silicon wafers, with or without Al_2O_3 covered, after diffusion treatment.

Photo (1). Phosphorous capsule diffusion. A. blank wafer; B. 1500 \AA Al_2O_3 covered; C. 3300 \AA Al_2O_3 covered.

Photo (2). Gallium capsule diffusion. A, B, C. Same as photo (1). D. 5300 \AA Al_2O_3 covered.

Photo (3). Boron capsule diffusion. A, B, C, D. Same as photo (2)

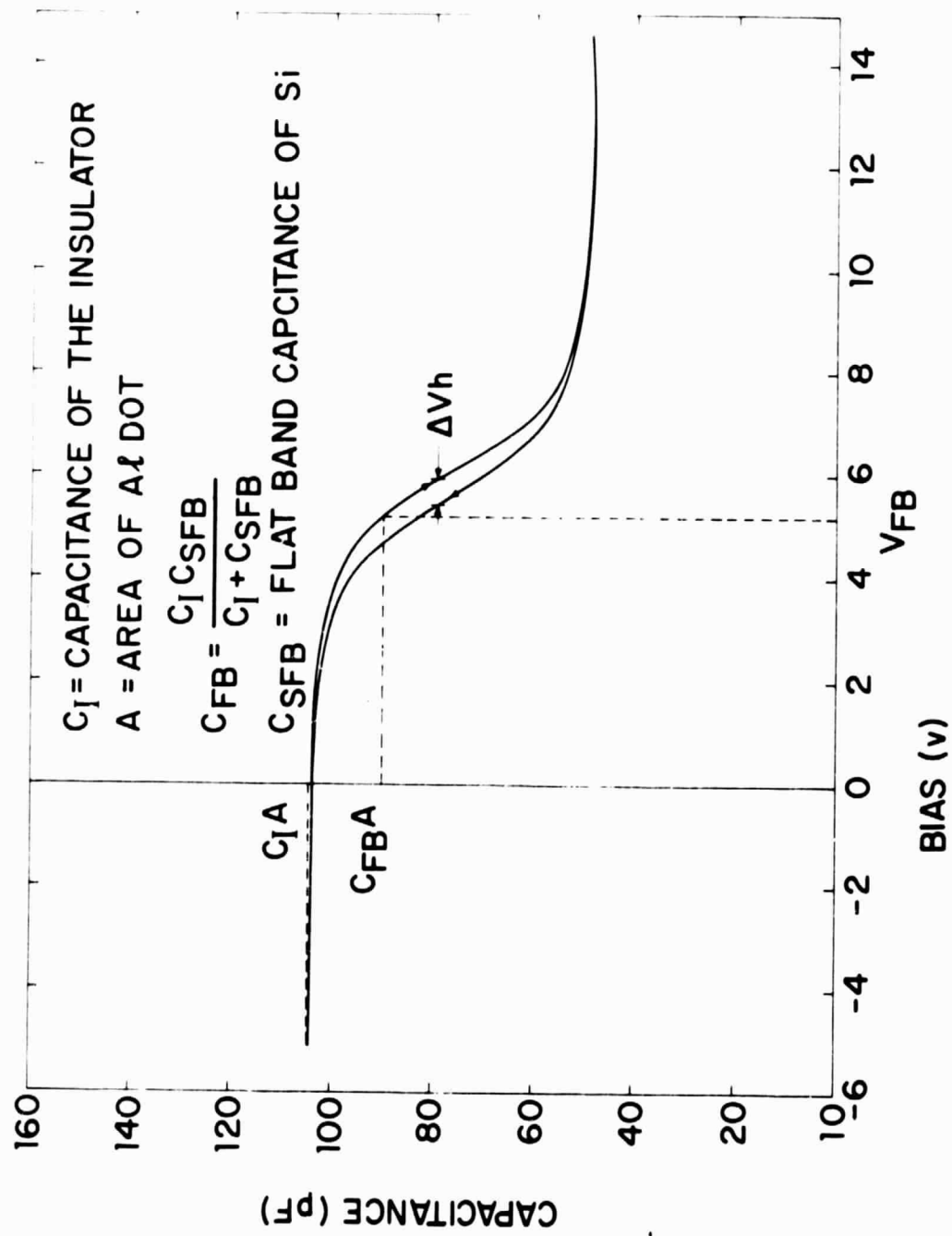


Fig. 7. A typical C-V curve of pyrolytic Al_2O_3 film ($900^\circ C$) on P⁻ 100 Si wafer.

Table I presents the calculated data of flat band charge densities N_{FB} of Al_2O_3 films deposited at temperatures from 750° to $1050^\circ C$. It appears that in the temperature range from $800^\circ C$ to $1050^\circ C$, N_{FB} is more or less dependent on substrate temperature. The positive flat band voltages are indicative of negative charges in the film and positive charge on the silicon surface. This so-called-"P-type invert" of the silicon surface is in agreement with the findings of Aboaf⁴ and of Matsushita and Koga.⁵

2.4.1.2 Effect of the Reactant Gas Composition

Table II summarizes the V_{FB} and N_{FB} data of the Al_2O_3 films deposited in a reactant gas containing different $CO_2/AlCl_3$ mole ratio. Since hydrogen was used as main carrier gas, any changes of $CO_2/AlCl_3$ mole ratio will correspondingly alter ion concentration of CO_2 in the gas phase, consequently affecting the kinetics of water formation.

As a predominant rate controlling factor for film growth, the kinetics of water formation may significantly affect film properties. This study was conducted at 750° and $900^\circ C$. Only limited data are available for comparison. It appears that at $750^\circ C$ there is no definite correlation between flat band charge density and the $CO_2/AlCl_3$ ratio varying from 145.1 to 310.1 (Table IIA). For films prepared at $900^\circ C$, N_{FB} increases steadily with increasing $CO_2/AlCl_3$ mole ratio (Table IIB). The charge density is generally related to the degree of film imperfection; films having more imperfection should exhibit greater charge density. This is probably true for Al_2O_3 films prepared with a large $CO_2/AlCl_3$ mole ratio.

2.4.2 Effect of the Main Carrier Gas on N_{FB}

Based on the experimental results, it was found that partial substitution of A for H_2 as the main carrier gas drastically reduced the N_{FB} of the MAS samples. As

TABLE I. Effect of Substrate Temperature on N_{FB}^{**} .

Sample	Wafer	Substrate Temp. (°C)	V_{FB} (V)	N_{FB} (1/cm ²)
A10-21-8	P ⁻ 100	750	+4.5	1.27×10^{12} *
A10-10-6	N ⁻ 111	800	+1.7	7.4×10^{11}
A10-15-6	N ⁻ 100	850	+2.92	8.4×10^{11}
A10-19-8	P ⁻ 100	950	+3.6	11.0×10^{11}
A10-17-6	P ⁻ 100	1050	+2.8	8.7×10^{11}

* C-V curve shifts readily at room temperature. The inaccuracy of N_{FB} is high for films deposited at 750°C.

** Flow rate: H₂ (main carrier gas) = 20 l/min, H₂/AlCl₃ = 150 cc/min., CO₂ = 400 cc/min.

TABLE II. Effect of $\text{CO}_2/\text{AlCl}_3$ Mole Ratio on N_{FB} .

A. Al_2O_3 Films Deposited at 750°C .

Sample	$\text{CO}_2/\text{AlCl}_3$	$V_{\text{FB}}(\text{V})$	$N_{\text{FB}}(1/\text{cm}^2)$
AIO-21-8	310	+4.5	$+12.7 \times 10^4$
AIO-22-6	248	-0.52	-1.82×10^4
AIO-23-6	205	-0.52	-1.80×10^4
AIO-24-6	154	-4.6	-17.0×10^4
AIO-25-6	145	-0.65	-2.0×10^4

B. Al_2O_3 Films Deposited at 900°C .

Sample	$\text{CO}_2/\text{AlCl}_3$	$V_{\text{FB}}(\text{V})$	$N_{\text{FB}}(1/\text{cm}^2)$
AIO-42-7	18.5	+1.95- +2.15	$+5.33- +5.85 \times 10^{11}$
AIO-65-7	24.6	+2.28	$+5.46 \times 10^{11}$
AIO-45-7	40.0	+1.95- +2.67	$+4.6- +5.92 \times 10^{11}$
AIO-46-7	49.3	+3.25- +3.8	$+6.2- +7.2 \times 10^{11}$
AIO-47-7	61.7	+3.9- +4.36	$+8.13- +9.2 \times 10^{11}$
AIO-48-7	92.5	+5.72- +6.11	$+1.3- +1.37 \times 10^{12}$
AIO-49-7	123.0	+0.65- +2.6	$+1.3- +4.94 \times 10^{12}$

shown in Table III, the N_{FB} of the MAS samples with the Al_2O_3 film deposited in a main carrier gas having H_2 content less than 15% is small ($10^{10}/cm^2$). When the H_2 content in the main carrier gas exceeded 20%, the N_{FB} of the Al_2O_3 film was increased one order of magnitude. The effect of the type of wafer on N_{FB} was also noticeable when A was used as the main carrier gas. Results strongly indicate that the Al_2O_3 film on P-type wafer has a smaller N_{FB} than that on a N-type wafer.

2.4.3 Flat Band Voltage and Charge Density of MAOS Samples

The flat band voltage and charge densities of MAOS samples were measured. The results are presented in Table IV. The composite layer of Al_2O_3 over low temperature pyrolytic SiO_2 exhibits the highest N_{FB} , while the Al_2O_3 over in-situ SiO_2 composite film has the lowest N_{FB} . With the exception of one sample, the flat band voltages of all the samples containing composite films of Al_2O_3 over thermally grown SiO_2 were negative. The charge density ranges from 2.0×10^{10} to $2.6 \times 10^{11} 1/cm^2$. As shown in Table IV-C, the turn-on voltage, V_T , of the composite film (Al_2O_3 over in-situ thermally grown SiO_2) is less than ± 1.0 volts. This makes Al_2O_3 films attractive for gate insulator application in FET devices.

2.4.4 Effect of Temperature-Bias Treatment

Results from preliminary study on the temperature-bias treatment of the Al_2O_3 and the Al_2O_3 over SiO_2 composite films reveal that, the V_{FB} and N_{FB} of the MAS change only with positive temperature bias, whereas the MAOS results are just the opposite (Table V).

2.4.5 Dielectric Constants and Electrical Strength

The dielectric constants, K , of Al_2O_3 films were calculated from the capacitance of the MAS measurements. With the exception of $800^\circ C$ deposited film where

TABLE III. Effect of A Carrier Gas on N_{FB} .

Sample	Wafer	Carrier Gas		V_{FB} (V)	N_{FB} (1/cm ²)
		H ₂ (%)	A(%)		
AIO-102-3	P ⁻ 100	15	85	-0.26 +0.14V	-6.8- +3.7 x 10 ¹⁰
AIO-103-5	P ⁻ 100	20	80	+2.6	+6.7 x 10 ¹¹
AIO-47-7	P ⁻ 100	100	0	+5.72 +6.11	+1.3- +1.37 x 10 ¹²
AIO-102-6	N ⁻ 100	15	85	-0.26 -0.45	-6.64- +1.15 x 10 ¹¹
AIO-103-4	N ⁻ 100	20	80	+4.5 +4.9	+1.2- +1.3 x 10 ¹²

Note: Deposition condition: substrate temperature = 900°C; H₂/AlCl₃ = 500 cc/min; CO₂ = 200 cc/min.

TABLE IV. V_{FB} and N_{FB} of MAOS (Metal- Al_2O_3 - SiO_2 -Si) Structures.

A. Al_2O_3 over Pyrolytic SiO_2 *.

Sample	Wafer	Film (\AA)		Sub. Temp. ($^{\circ}C$)	$V_{FB}(V)$	$N_{FB}(1/cm^2)$
		SiO_2	Al_2O_3			
AIO-88	P ⁻ 100	1200	1000	900	-7.0	-1.3×10^{12}
AIO-60-5	P ⁻ 100	1900	1000	1050	+4.6	$+7.0 \times 10^{11}$

* Deposition temperature $475^{\circ}C$.

B. Al_2O_3 thermally SiO_2 .

Sample	Wafer	Film (\AA)		Sub. Temp. ($^{\circ}C$)	$V_{FB}(V)$	$N_{FB}(1/cm^2)$
		SiO_2	Al_2O_3			
AIO-40	N ⁻ 100	4000	1200	900	+0.25	$+2.1 \times 10^{10}$
AIO-55-7	P ⁻ 100	4000	1200	900	-2.6	-2.6×10^{11}
AIO-65-4	N ⁻ 100	500	2000	900	-1.3	-1.5×10^{11}
AIO-65-2	N ⁻ 100	1000	2300	900	-1.95	-1.8×10^{11}
AIO-86-9	N ⁻ 100	4500	1500	900	-3.3	-2.6×10^{11}
AIO-87-5	N ⁻ 100	780	1500	900	-1.04	-2.0×10^{11}

C. Al_2O_3 over in-situ SiO_2 * (substrate temperature $900^{\circ}C$)

Sample	Wafer	Film (\AA)		$V_T(V)$	$V_{FB}(V)$	$N_{FB}(1/cm^2)$
		SiO_2	Al_2O_3			
AIO-91-2	P ⁻ 100	500	500	+0.6	-0.2	$+4.76 \times 10^{10}$
AIO-91-5	P ⁻ 111	500	500	+0.01	-0.4	-1.05×10^{11}
AIO-94-3	P ⁻ 100	500	3000	+1.5	-0.3	-4.4×10^{10}
AIO-94-4	P ⁻ 111	500	3000	-1.6	-2.4	-3.4×10^{11}
AIO-95-5	P ⁻ 100	1000	500	+0.4	-0.14 +0.12	$-2.8- +2.0 \times 10^{10}$
AIO-95-3	P ⁻ 100	1000	500	+0.01	-0.52	-9.5×10^{10}

* Dry oxygen at $1000^{\circ}C$.

TABLE V. Effect of Temperature-Bias Treatment.

Sample	Wafer	Film (Å)		Temp. Bias	$V_{FB}(V)$	$N_{FB}(1/cm^2)$
		SiO ₂	Al ₂ O ₃			
AIO-65-7	N ⁻	100	0	2000	-	0
					+	-3.04
AIO-65-4	N ⁻	100	500	2000	-	$+6.2 \times 10^{11}$
					+	0
AIO-65-2	N ⁻	100	1000	2300	-	-1.6×10^{11}
					+	0

Note: "-" -30 volts at 300°C for 30 min.

$K = 20$, the dielectric constants of Al_2O_3 films are in the range of 6.8 to 11.0 and appear to be independent on the deposition temperature. The variation in K values of Al_2O_3 film might be attributed to the difference in degree of preferential orientation and the extent of crystal imperfections. The electrical breakdown strength of the Al_2O_3 films is approximately 9×10^6 /cm or higher. This breakdown strength does not appear to bear any quantitative relationship with the substrate temperatures.

3.0 NEW TECHNOLOGY

In the previous technology, H_2 was used as the main carrier gas for diluting the active reactant, AlCl_3 . Al_2O_3 films thus prepared were generally found to exhibit high flat band charge density. Under the newly developed technology of using A to replace H_2 as the main carrier gas, the flat band charge density of the Al_2O_3 was reduced substantially. The improvement of film properties is attributed to the use of this new technology.

4.0 FUTURE WORK

The future work for this contract will include the following:

- A. Analyze the chemical composition of Al_2O_3 films,
- B. Conduct studies in Al_2O_3 deposition on B_2O_3 - SiO_2 precoated silicon wafers,
- C. Conduct studies on Al_2O_3 deposition on P_2O_5 - SiO_2 precoated silicon wafers,
- D. Determine the masking capability of Al_2O_3 film against Na diffusion.
- E. Continue the electrical property measurements and evaluation, and
- F. Prepare test insulated gate-field effect transistors leading to the fabrication of a simple integrated circuit array.

5.0 ACKNOWLEDGEMENTS

Portions of the work in this report were contributed by Joseph C. Hollis, Arthur G. Smith, Elmar K. Brandis, William D. Rosenberg, George A. Walker, Joseph Woods and Richard A. Baker, Jr.

6.0 REFERENCES

1. A. S. Grove, B. E. Deal, E. H. Snow and C. T. Sah, *Solid State Electronics* 8, 145 (1965).
2. First Quarterly Report, this contract September 1968.
3. NASA Contract Report NASA CR-995.
4. J. A. Aboaf, *J. Electro Chem. Soc.* 114, 948 (1967).
5. M. Matusshita and Y. Koga, *Electrochem. Soc. Meeting*, Spring 1968, Abstract No. 90.